



Letter

pubs.acs.org/acscatalysis

Formation of Alkanes by Aerobic Carbon–Carbon Bond Coupling Reactions Catalyzed by a Phosphovanadomolybdc Acid

Miriam Somekh,[†] Hagai Cohen,[‡] Yael Diskin-Posner,[‡] Linda J. W. Shimon,[‡] Raanan Carmieli,[‡] Jeffrey N. Rosenberg,^{†,§} and Ronny Neumann^{*,†,§}

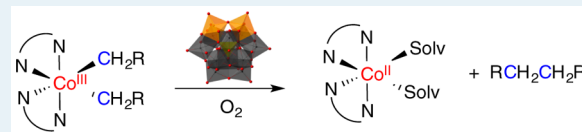
[†]Department of Organic Chemistry, Weizmann Institute of Science, Rehovot 76100, Israel

[‡]Department for Chemical Research Support, Weizmann Institute of Science, Rehovot 76100, Israel

S Supporting Information

ABSTRACT: The valorization of alkanes is possible via carbon–carbon coupling reactions. A series of dialkyl cobalt complexes $[(RCH_2)_2Co^{III}(bpy)_2]ClO_4$ ($R = H, Me, Et, \text{ and } Ph$) were reacted with the $H_5PV_2Mo_{10}O_{40}$ polyoxometalate as a catalyst, leading to a selective oxidative carbon–carbon bond coupling reaction. The reaction is initiated by electron transfer from $[(RCH_2)_2Co^{III}(bpy)_2]^+$ to $H_5PV_2Mo_{10}O_{40}$ to yield an intermediate $[(RCH_2)_2Co^{IV}(bpy)_2]^{2+}-H_5PV^{IV}V_2Mo_{10}O_{40}$, as identified by a combination of EPR and X-ray photoelectron spectroscopy experiments. The reaction is catalytic with O_2 as terminal oxidant representing an aerobic C–C bond coupling reaction.

KEYWORDS: aerobic oxidation, C–C bond coupling, polyoxometalate, XPS, electron transfer



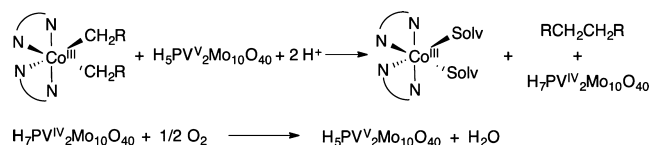
INTRODUCTION

Oxidative sp^3-sp^3 C–C bond coupling reactions of metal–dialkyl compounds through an oxidative reductive elimination pathway is quite well-known. For example, early work by Kochi and colleagues showed that thermolysis of $Et_2Fe(bpy)_2$ yielded ethene and ethane, products of β -hydrogen elimination; however, a two-electron oxidation process led to selective reductive elimination and formation of *n*-butane only.¹ More recent research has been focused on square planar Pd(II) compounds where reactions proceed via higher valent Pd(III) or Pd(IV) intermediates.² Such reactions have much present relevance also in the context of valorization of light alkanes, especially methane. Recently, there have been some reports on similar intermolecular C–C bond coupling reactions from both Pd(II) and Ni(II) square planar precursors.³ Generally speaking, oxidation at the metal center has been achieved by using both one- and two-electron stoichiometric oxidants, often in excess. The use of ferrocenium cations,⁴ Ag^+ ,⁵ benzoquinone,⁶ and pyridinium compounds,⁷ among others, is notable.

Surprisingly, the use of O_2 as terminal oxidant has not been shown for the oxidative coupling reactions mentioned above. To facilitate such a transformation, a one- or two-electron oxidant to the metal–dialkyl species that could be then recovered by reoxidation with O_2 would be very advantageous toward an aerobic catalytic transformation. Indeed, it has been shown in the past that phosphovanadomolybdates of the α -Keggin structure such as $H_5PV_2Mo_{10}O_{40}$ are excellent electron-transfer oxidants of many substrate types that upon reduction by one or two electrons are quite easily reoxidized by O_2 .⁸ It should be specifically noted that tetra-alkyltin compounds also can be activated and aerobically oxidized with $H_5PV_2Mo_{10}O_{40}$, but in that case, oxygen insertion into the metal–carbon bond

occurs to yield an alcohol as the product.⁹ In the research presented in this paper, we demonstrate such an aerobic oxidative C–C bond coupling reaction with dialkyl cobalt(III) substrates (Scheme 1).

Scheme 1. Aerobic Oxidative C–C Bond Formation in Dialkylcobalt(III) Compounds Catalyzed by $H_5PV_2Mo_{10}O_{40}$



RESULTS AND DISCUSSION

A series of dialkyl cobalt complexes $[(RCH_2)_2Co^{III}(bpy)_2]ClO_4$ where $R = H$ (**1a**), CH_3 (**1b**), CH_3CH_2 (**1c**), Ph (**1d**), and for cyclic- $CH_2CH_2CH_2CH_2$ (**1e**) was synthesized by adaptation of a literature method that involves the in situ reductive alkylation of a Co(II) salt in the presence of 2,2'-bipyridine, $NaBH_4$ and the appropriate alkyl halide.¹⁰ The red complexes that were obtained were diamagnetic. Crystal structures were obtained for **1c,d** (Figure 1) and **1e** (Figure S11).

The crystal structures revealed the expected six-coordinate regular octahedral complex with the alkyl moieties in the α -cis positions. We were unable to crystallize complexes **1a–b**; however, they were unequivocally identified by their NMR spectra (see the Supporting Information).

Received: February 12, 2017

Revised: March 8, 2017

Published: March 14, 2017

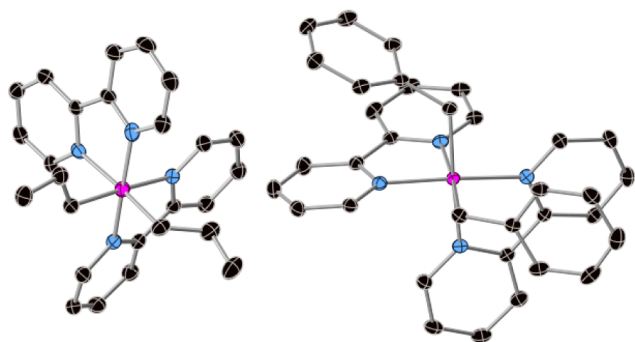


Figure 1. ORTEP drawing (50% probability) of **1c** (left) and **1d** (right). Co, magenta; C, black; and N, blue. Hydrogen atoms and the ClO₄ anion are not shown.

After preparation of **1a–e**, they were each reacted with an equivalent amount of H₅PV₂Mo₁₀O₄₀ as oxidant under Ar. Thus, 30 μmol of **1** and 30 μmol of H₅PV₂Mo₁₀O₄₀ in 6 mL of *n*-butyronitrile were reacted at RT. Immediately, a blue precipitate of the signature heteropoly blue compound was formed signifying that the polyoxometalate was instantaneously reduced. Analysis of the reaction mixture at this point showed no significant formation of product, indicating that the precipitate is a reaction intermediate (see below). Subsequent heating of the solution at 50 °C for 3 h revealed the quantitative formation of ethane, *n*-butane, *n*-hexane, bibenzyl, and cyclobutane for **1a–e**, respectively. No oxygen transfer from the polyoxometalate by an ET-OT mechanism⁸ to obtain an oxygenated product such as RCH₂OH was observed, as occurred with Sn(alkyl)₄ substrates.⁹ Rather, the results point to a highly selective head-to-head oxidative carbon–carbon coupling with no formation of byproducts. For example, from **1c**, no propane, propene, acetone, or other hexane isomers were formed. A control experiment without H₅PV₂Mo₁₀O₄₀ showed that **1** was stable under the reaction conditions. Only upon heating to 220 °C was a mixture of products formed. Similar stoichiometric reactions of **1** and H₅PV₂Mo₁₀O₄₀ under 1.5 bar O₂ also yielded only the C–C coupling products except for **1d** (R = Ph) where both benzaldehyde (83%) and bibenzyl (17%) were formed in a quantitative reaction. Since oxygen transfer from the polyoxometalate was not observed for **1a–e**, one can conclude that for **1d** only, O₂ directly reacted with an intermediate to yield benzaldehyde. This was confirmed by carrying out a reaction with ¹⁸O₂ that yielded PhCH¹⁸O.

Since it is known, as discussed above, that the reduced polyoxometalate, that is, H₇PV^{IV}₂Mo₁₀O₄₀, can be oxidized to H₅PV^V₂Mo₁₀O₄₀ with O₂, catalytic reactions were carried out as summarized in Table 1. As seen in Table 1, the reaction products were identical to those obtained in the stoichiometric

Table 1. Aerobic Catalytic C–C Bond Coupling^a

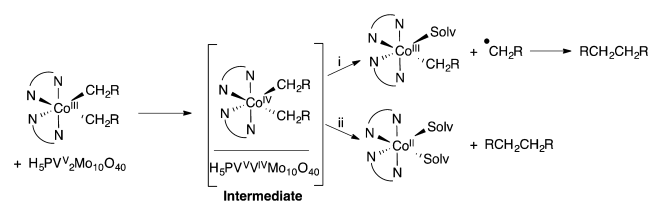
| substrate | product | yield, mol % | TON |
|---------------------------------|-----------------------|--------------|-----|
| 1a (R = H) | 100% ethane | 61 | 35 |
| 1b (R = Me) | 100% <i>n</i> -butane | 64 | 37 |
| 1c (R = Et) | 100% <i>n</i> -hexane | 66 | 38 |
| 1c (R = Et) ^b | 100% <i>n</i> -hexane | 100 | 58 |
| 1d (R = Ph) | 89% PhCHO, 11% Bz-Bz | 64 | 37 |

^aReaction conditions: 150 μmol of **1a–d**, 2.6 μmol of H₅PV₂Mo₁₀O₄₀, 15 mL of *n*-butyronitrile, 5 bar of O₂, 24 h, 60 °C. ^b4 μmol of H₂SO₄ added, 12 h.

reactions under O₂. Furthermore, the yields and turnover numbers were very similar for all substrates, suggesting that in these reactions the rate-determining step for the catalytic reaction is the reoxidation of H₇PV^{IV}₂Mo₁₀O₄₀ with O₂. Note that since in the oxidative reductive elimination process no protons are formed, their addition considerably improves the efficiency of the reoxidation reaction in the catalytic cycle (third entry); see also Scheme 1.¹¹

After demonstrating selective aerobic catalytic C–C bond coupling, we turned our attention to the reaction mechanism and the identification of the apparent reaction intermediate, the blue precipitate. Given that H₅PV₂Mo₁₀O₄₀ reacts with **1** to create a more electron-poor metal center via electron transfer, two realistic reaction mechanisms can be contemplated: (i) Co–alkyl bond homolysis and (ii) direct reductive elimination (Scheme 2).

Scheme 2. Pathways for C–C Bond Coupling of **1** with H₅PV₂Mo₁₀O₄₀



The Co–alkyl bond homolysis can be excluded as such a pathway and would likely yield various alkane isomers because one could expect stabilization of secondary carbon radicals versus primary ones. Thus, for alkyl = *n*-propyl, 2,3-dimethylbutane would be a more likely product compared to the *n*-hexane. The formation of propane would also be possible in such a case by a hydrogen-atom-transfer step. In addition, a crossover experiment where a 1:1 ratio of RCH₂ = Et and *n*-Pr were used as substrates, only *n*-butane and *n*-hexane were formed with no pentane product whatsoever. Disproportionation (not shown) was the likely pathway for oxidative C–C bond coupling from square planar Pd(II) and Pt(II) complexes,^{2a,12} however, this seems very unlikely in this case because this would require the formation of a heptacoordinate Co(V) complex and a Co(III) complex from an initially formed Co(IV) intermediate. Furthermore, a crossover experiment as mentioned above would be expected to yield butane, pentane, and hexane in a 1:2:1 ratio. Thus, the results would appear to support a direct reductive elimination pathway as the most reasonable option to explain the high selectivity of the reaction.

A qualitative determination of the blue intermediate species obtained from an equimolar mixture of **1c** and H₅PV₂Mo₁₀O₄₀ as portrayed in Scheme 2 can be obtained by low-temperature X-band EPR spectroscopy, Figure 2. One can discern two peaks: the typical anisotropic spectrum at *g* = ~2.1 for a vanadium(IV) species associated with the one-electron reduced polyoxometalate¹³ and a peak at *g* = ~4.3 that we associate with a small amount of a *S* = 3/2 Co(II) species that is formed in the reaction (see below).¹⁴ A peak assignable to Co(IV) is not apparent.¹⁴ Under conditions where the intermediate is let to react in the solid state, the peak associated with the *S* = 3/2 Co(II) species is more significant (Figure S15).

Despite the obvious redox reaction between **1c** and H₅PV₂Mo₁₀O₄₀ and the formation of V(IV) as shown by EPR, and because the peak associable to Co(IV) was not

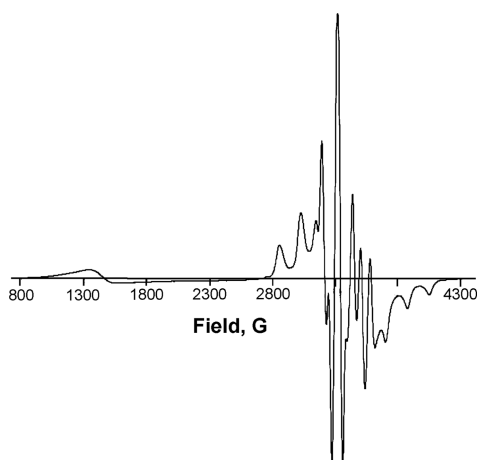


Figure 2. X-band EPR spectrum of the intermediate species.

observed, we turned to XPS measurements to obtain further information and to quantitatively decipher the cobalt and vanadium species as a function of their oxidation states. Thus, **1c** and $\text{H}_5\text{PV}_2\text{Mo}_{10}\text{O}_{40}$ were reacted in a 1:1 ratio. The blue precipitate that was formed was immediately vacuum filtered, dried under high vacuum, transferred to a carbon tape, and promptly taken to the spectrometer to minimize air exposure of the sample. Compounds **1c** and $[\text{Co}^{\text{II}}(\text{bpy})_2(\text{CH}_3\text{CN})_2]\text{Cl}_2$ were used as references for cobalt(III) and cobalt(II),¹⁵ respectively. $\text{H}_5\text{PV}_2\text{Mo}_{10}\text{O}_{40}$ was used as a reference for vanadium(V). The X-ray photoelectron spectroscopy (XPS) $\text{Co } 2p_{3/2}$ line of the intermediate and the control compounds for Co(II) and Co(III) are presented in Figure 3, left. The first

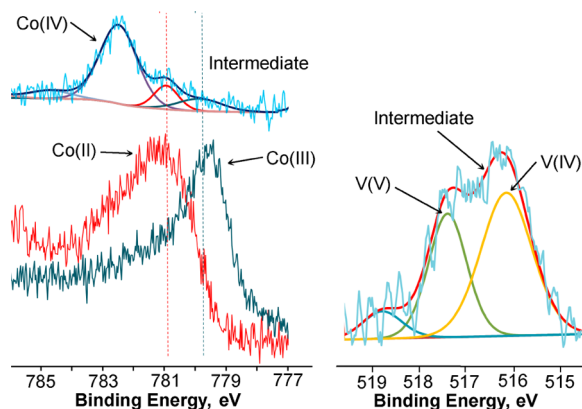


Figure 3. X-ray photoelectron spectra of the reaction intermediate, **1c**, and reference compound, $[(\text{Solv})_2\text{Co}^{\text{II}}(\text{bpy})_2]\text{Cl}_2$. Left: the $\text{Co } 2p_{3/2}$ spectral window. Right: the $\text{V } 2p_{3/2}$ line.

point of note is that, unusually, the Co(II) compound has a higher binding energy, 780.9 eV, than the Co(III) compound, 779.7 eV, which is opposite to the general trend of chemical shifts in XPS; the general trend is the higher the oxidation state, the higher the binding energy. This phenomenon has already been reported and explained by the presence of strong electron interactions: the occupied d_{z^2} valence orbital in Co(II) increases the binding energy,¹⁶ while the absence of an electron in the valence orbital of Co(III) leads to a lower binding energy, despite the higher oxidation state. Clearly, the intermediate has a significantly higher binding energy, 782.5 eV, see Figure 3, than the two reference samples. It is assigned

to a Co(IV) metal center. Notably, additional Co(II) and Co(III) are found as well in this case, and this finding is discussed below.

In Figure 3, right, we present the XPS $\text{V } 2p_{3/2}$ line of the intermediate. As would be expected for a one-electron transfer process, the reaction of **1c** and $\text{H}_5\text{PV}^{\text{V}}_2\text{Mo}_{10}\text{O}_{40}$ should yield an intermediate containing $[\text{PV}^{\text{IV}}\text{V}^{\text{V}}\text{Mo}_{10}\text{O}_{40}]^{6-}$ that would have an equimolar amount of V(IV) and V(V). Figure 3 suggests that this is approximately though not exactly correct. The measured higher amount of V(IV) versus V(V) and the small amounts of Co(II) and even Co(III) can be attributed to impurities in the intermediate, which is due to its further reaction under the vacuum conditions and low-flux X-ray irradiation to yield *n*-hexane and a Co(II) compound by reductive elimination (Scheme 2). The latter can then be oxidized by the polyoxometalate to yield a Co(III) compound and more V(IV) species, thus explaining all the experimental XPS results.

CONCLUSION

An aerobic oxidative catalytic C–C bond coupling reaction of an octahedral dialkyl–cobalt(III) complex, $[(\text{RCH}_2)_2\text{Co}^{\text{III}}(\text{bpy})_2]^+$, yielded the head-to-head product only, for example, *n*-hexane from $\text{R} = \text{Et}$. The reaction was shown to take place by using $\text{H}_5\text{PV}^{\text{V}}_2\text{Mo}_{10}\text{O}_{40}$ as an electron-transfer catalyst, forming a $[(\text{RCH}_2)_2\text{Co}^{\text{IV}}(\text{bpy})_2]^{2+} - \text{H}_5\text{PV}^{\text{IV}}\text{V}^{\text{V}}\text{Mo}_{10}\text{O}_{40}$ intermediate at room temperature. By heating to 50 °C, the C–C bond coupling takes place through a reductive elimination step. For $\text{RCH}_2 = \text{Bz}$, oxygenation also occurs in significant amounts in a kinetically competitive reaction. The working hypothesis is that O_2 can react with the reduced polyoxometalate in the intermediate to yield a superoxide ($\text{V}^{\text{V}}-\text{OO}\cdot$), which leads to oxygenation and formation of the aldehyde. Interestingly, the EPR spectrum indicates that the Co(II) species formed is high spin, $S = 3/2$. This species is reoxidized to yield a diamagnetic Co(III) species and $\text{H}_5\text{PV}^{\text{IV}}_2\text{Mo}_{10}\text{O}_{40}$. Since the latter is easily oxidized in the presence of protons and O_2 as terminal oxidant, catalytic turnover is observed under aerobic conditions, a novel finding in this area where the use of one- and two-electron stoichiometric oxidants is the norm. Future research will be focused on combining alkane activation with oxidative C–C bond coupling as described.

EXPERIMENTAL SECTION

Synthesis of Complexes 1a–d. An orange deaerated solution of 0.78 g (5 mmol) of 2,2-bipyridine and 0.60 g (2.5 mmol) of $\text{CoCl}_2 \cdot 6\text{H}_2\text{O}$ in 50 mL of methanol was prepared, and then the corresponding alkyl halide (7.5 mmol RI; $\text{R} = \text{Me}$ Et, *n*-Pr or 5.0 mmol BzCl) was added to the solution under a slight positive pressure of Ar. NaBH_4 (0.2 g, 5 mmol) was added under vigorous stirring in small portions during a period of 40 min. After every addition of NaBH_4 , a blue Co(I) intermediate was formed. The next portion was added only after the blue color disappeared. After a few portions, the solution slowly became dark red. Note that an excess of NaBH_4 needs to be avoided. The red solution was treated with 0.3 g of NaClO_4 dissolved in 10 mL of water followed by evaporation to 15 mL. Addition of 30 mL of cold H_2O yielded a precipitate that was collected by centrifugation. The precipitate was washed with cold water until the wash was almost colorless. Water was removed by lyophilization, and the products were

stored at $-80\text{ }^{\circ}\text{C}$. ^1H NMR and ^{13}C NMR were recorded on Bruker Avance 300 and 500 MHz spectrometers at 298 K and referenced to solvent shift. The NMR and HR-MS spectra of **1a–d**, and their analysis can be found in the [Supporting Information](#).

Synthesis of Complex 1e. An orange deaerated solution of 0.78 g (5.0 mmol) of 2,2-bipyridine and 0.60 g (2.5 mmol) of $\text{CoCl}_2\cdot 6\text{H}_2\text{O}$ in 30 mL of methanol and 20 mL of dimethoxy ethane was prepared, and then 0.2 g (0.625 mmol) of 1,4-diiodobutane was added. The solution was deaerated for 15 min with Ar, and then 2.5 mmol of NaBH_4 was added as described above and left to react for an additional 20 min. Next, 0.3 g (2.5 mmol) of the product was isolated as described above. Note that the use of 1.25 mmol of 1,4-diiodobutane yielded a dialkyl complex with two iodo-butane ligands and not the metallocycle. This compound also underwent C–C coupling to yield 1,8-diiodooctane.

X-ray Crystallography. Samples (10 mg) were dissolved in 1 mL of CH_3CN in a 2 mL vial. The open vial was inserted in a 20 mL vial with 3 mL of diethyl ether. The bigger vial was tightly closed and left for 2 weeks at $4\text{ }^{\circ}\text{C}$. Single-crystal X-ray data were collected on a Bruker APEX-II Kappa CCD or Rigaku XtaLab PRO equipped with PILATUS 200 diffractometer with Mo $K\alpha$ ($\lambda = 0.71073\text{ nm}$) radiation and graphite monochromator. Measurements were performed at 100 K under liquid N_2 to achieve better -quality data. The data were processed using Bruker Apex2 suite for complex **1c** and **1d**, and CrysAlisPro 1.171.39.4c for **1e**. Structures were solved by direct methods with SHELXS or SHELXT. Full-matrix least-squares refinement was based on F^2 with SHELXL-2014. The crystallographic data are presented in [Table S1](#).

X-ray Photoelectron Spectroscopy. Compound **1c** and $\text{H}_5\text{PV}_2\text{Mo}_{10}\text{O}_{40}$ were reacted at a 1:1 ratio. The blue precipitate that was formed was immediately vacuum filtered, dried under high vacuum, transferred to a carbon tape, and promptly taken to the spectrometer to minimize oxygen exposure of the sample. Measurements were performed in a Kratos AXIS-Ultra DLD spectrometer at a base pressure of 10^{-9} Torr, using monochromatic Al $K\alpha$ source at a highly reduced power, up to 15 W at the most. Charge compensation by an electron flood gun was needed in all measurements of these powders. Given the large spot-dependent charging variations and small yet important binding energy chemical shifts in the organic species, we used the two leading C 1s lines of the bipyridine ligands for energy-scale calibration (cross checked with the bipyridine nitrogen and with the Mo 3d of the polyoxometalate signal). This referencing procedure reduced the uncertainty in binding energies to values much smaller than the differences observed in the Co line. Particular care was taken in our procedures because sample degradation occurs under X-ray irradiation; as such, we used extremely low fluxes and repeated scans in order to follow those processes and eventually extract the data under minimally damaging conditions.¹⁷

EPR Spectroscopy. Compound **1c** and $\text{H}_5\text{PV}_2\text{Mo}_{10}\text{O}_{40}$ were reacted at a 1:1 ratio, the blue precipitate that was formed was immediately transferred into an EPR capillary tube and analyzed on the spot. X-band EPR spectra were recorded on a Bruker ELEXSYS 500 spectrometer equipped with a Bruker ER4122SHQE resonator at 20 K with microwave power of 20 mW, 0.1 mT modulation amplitude and 100 kHz modulation frequency.

Carbon–Carbon Coupling Reactions. Stoichiometric reactions: **1a–e** (30 μmol) and 30 μmol (69 mg) of

$\text{H}_5\text{PV}_2\text{Mo}_{10}\text{O}_{40}\cdot 32\text{H}_2\text{O}$ ¹⁸ each in 3 mL of *n*-butyronitrile were mixed in an Ace glass pressure tube and then frozen, degassed, and filled with 1.5 atm of Ar or O_2 . The mixture was stirred at $50\text{ }^{\circ}\text{C}$ for 3 h, cooled to $\sim 0\text{ }^{\circ}\text{C}$, and analyzed by gas chromatography. Catalytic reactions: **1a–d** (150 μmol) were reacted with 2.6 μmol (6 mg) of $\text{H}_5\text{PV}_2\text{Mo}_{10}\text{O}_{40}\cdot 32\text{H}_2\text{O}$ in 15 mL of *n*-butyronitrile for 24 h at $60\text{ }^{\circ}\text{C}$ under 5 bar O_2 . Gas phases were analyzed by GC-TCD equipped with a 2 m, 0.53 μm i.d. Restek ShinCarbon ST 80/100 column and quantified using standards. Liquids were qualitatively analyzed GC-MS and quantified by GC-FID for quantitative analysis using a Restek 5% phenyl methylsilicone 0.32 mm i.d., 0.25 mm coating, 30 m column with He as carrier gas.

■ ASSOCIATED CONTENT

Supporting Information

The Supporting Information is available free of charge on the ACS Publications website at DOI: [10.1021/acscatal.7b00461](https://doi.org/10.1021/acscatal.7b00461).

Crystallographic data, additional NMR data, ORTEP drawing, high-resolution ESI-MS, X-band EPR spectrum (PDF)

X-ray data (CIF)

X-ray data (CIF)

X-ray data (CIF)

■ AUTHOR INFORMATION

Corresponding Author

*E-mail: Ronny.Neumann@weizmann.ac.il.

ORCID

Ronny Neumann: [0000-0002-5530-1287](https://orcid.org/0000-0002-5530-1287)

Present Address

[§](J.N.R.) Department of Chemistry, California Institute of Technology, Pasadena, CA 91125, United States. E-mail: jrosenbe@caltech.edu

Author Contributions

The manuscript was written through contributions of all authors and they have given their approval to the final version of the manuscript.

Notes

The authors declare no competing financial interest.

■ ACKNOWLEDGMENTS

This research was supported by the Israel Science Foundation (grant no. 2046/14). Bidyut B. Sarma is thanked for his assistance. R.N. is the Rebecca and Israel Sieff Professor of Organic Chemistry.

■ REFERENCES

- (1) Tsou, T. T.; Kochi, J. K. *J. Am. Chem. Soc.* **1978**, *100*, 1634–1635.
- (2) (a) Lanci, M. P.; Remy, M. S.; Kaminsky, W.; Mayer, J. M.; Sanford, M. S. *J. Am. Chem. Soc.* **2009**, *131*, 15618–15620. (b) Lanci, M. P.; Remy, M. S.; Lao, D. B.; Sanford, M. S.; Mayer, J. M. *Organometallics* **2011**, *30*, 3704–3707. (c) Khusnutdinova, J. R.; Rath, N. R.; Mirica, L. M. *J. Am. Chem. Soc.* **2012**, *134*, 2414–2422. (d) Byers, P. K.; Canty, A. J.; Skelton, B. W.; White, A. H. *J. Chem. Soc., Chem. Commun.* **1986**, 0, 1722–1724. (e) Byers, P. K.; Canty, A. J.; Crespo, M.; Puddephatt, R. J.; Scott, J. D. *Organometallics* **1988**, *7*, 1363–1367. (f) Duecker-Benfer, C.; van Eldik, R.; Canty, A. J. *Organometallics* **1994**, *13*, 2412–2414. (g) Canty, A. J. *Dalton Trans.* **2009**, 10409–10417. (h) Khusnutdinova, J. R.; Qu, F.; Zhang, Y.; Rath, N. P.; Mirica, L. M. *Organometallics* **2012**, *31*, 4627–4630.

- (i) Tang, F.; Zhang, Y.; Rath, N. P.; Mirica, L. M. *Organometallics* **2012**, *31*, 6690–6696.
- (3) (a) Lotz, M. D.; Remy, M. S.; Lao, D. B.; Ariafard, A.; Yates, B. F.; Canty, A. J.; Mayer, J. M.; Sanford, M. S. *J. Am. Chem. Soc.* **2014**, *136*, 8237–8242. (b) Xu, H.; Diccianni, J. B.; Katigbak, J.; Hu, C.; Zhang, Y.; Diao, T. *J. Am. Chem. Soc.* **2016**, *138*, 4779–4786.
- (4) Sato, M.; Mogi, E.; Kumakura, S. *Organometallics* **1995**, *14*, 3157–3159.
- (5) (a) Kraatz, H. B.; van der Boom, M. E.; Ben-David, Y.; Milstein, D. *Isr. J. Chem.* **2001**, *41*, 163–172. (b) MacLeod, K. C.; Patrick, B. O.; Smith, K. M. *Organometallics* **2012**, *31*, 6681–6689.
- (6) Albéniz, A.; Espinet, P.; Martín-Ruiz, B. *Chem. - Eur. J.* **2001**, *7*, 2481–2489.
- (7) Ball, N. D.; Kampf, J. W.; Sanford, M. S. *J. Am. Chem. Soc.* **2010**, *132*, 2878–2879.
- (8) (a) Neumann, R. *Inorg. Chem.* **2010**, *49*, 3594–3601. (b) Neumann, R.; Khenkin, A. M. *Chem. Commun.* **2006**, 2529–2538.
- (9) Khenkin, A. M.; Efremenko, I.; Martin, J. M. L.; Neumann, R. *J. Am. Chem. Soc.* **2013**, *135*, 19304–19310.
- (10) Mestroni, G.; Camus, A.; Mestroni, E. *J. Organomet. Chem.* **1970**, *24*, 775–781.
- (11) In a reaction cycle including alkane activation, the needed protons would come from the activation step.
- (12) Johansson, L.; Ryan, O. B.; Romming, C.; Tilset, M. *Organometallics* **1998**, *17*, 3957–3966.
- (13) (a) Kaminker, I.; Goldberg, H.; Neumann, R.; Goldfarb, D. *Chem. - Eur. J.* **2010**, *16*, 10014–10020. (b) Goldberg, H.; Kaminker, I.; Goldfarb, D.; Neumann, R. *Inorg. Chem.* **2009**, *48*, 7947–7952.
- (14) (a) McAlpin, J. G.; Surendranath, Y.; Dinca, M.; Stich, T. A.; Stoian, S. A.; Casey, W. H.; Nocera, D. G.; Britt, R. D. *J. Am. Chem. Soc.* **2010**, *132*, 6882–6883. (b) Jiménez, H. R.; Salgado, J.; Moratal, J. M.; Morgenstern-Badarau, I. *Inorg. Chem.* **1996**, *35*, 2737–2741.
- (15) Sobkowiak, A.; Sawyer, D. T. *J. Am. Chem. Soc.* **1991**, *113*, 9520–9523.
- (16) (a) Burger, K.; Furlani, C.; Mattogno, G. *J. Electron Spectrosc. Relat. Phenom.* **1980**, *21*, 249–256. (b) Ivanova, T.; Naumkin, A.; Sidorov, A.; Ereminenko, I.; Kiskin, M. *J. Electron Spectrosc. Relat. Phenom.* **2007**, *156–158*, 200–203.
- (17) Frydman, E.; Cohen, H.; Maoz, R.; Sagiv, J. *Langmuir* **1997**, *13*, 5089–5106.
- (18) Tsigidinos, G. A.; Hallada, C. J. *Inorg. Chem.* **1968**, *7*, 437–441.